

RSC Advances



This is an *Accepted Manuscript*, which has been through the Royal Society of Chemistry peer review process and has been accepted for publication.

Accepted Manuscripts are published online shortly after acceptance, before technical editing, formatting and proof reading. Using this free service, authors can make their results available to the community, in citable form, before we publish the edited article. This *Accepted Manuscript* will be replaced by the edited, formatted and paginated article as soon as this is available.

You can find more information about *Accepted Manuscripts* in the [Information for Authors](#).

Please note that technical editing may introduce minor changes to the text and/or graphics, which may alter content. The journal's standard [Terms & Conditions](#) and the [Ethical guidelines](#) still apply. In no event shall the Royal Society of Chemistry be held responsible for any errors or omissions in this *Accepted Manuscript* or any consequences arising from the use of any information it contains.

Near-Superhydrophobic Surface Reduces Hemolysis of Blood

Flow in Tubes

Chang Quan Lai^{1,2*}, Joel Chia Wei Shen³, Wilson Chua Wei Cheng³, Choon Hwai Yap²

¹*ETH Zürich, Tannenstrasse 3, CLA J 33, Zürich, Switzerland 8092*

²*Department of Biomedical Engineering, National University of Singapore, 7 Engineering Drive 1 Singapore 117574*

³*NUS High School of Mathematics and Science, 20 Clementi Ave 1, Singapore 129957*

Keywords: Superhydrophobic, Cassie, Hemodialysis, Hemolysis, Circulation, Shear, Microstructures, Nanostructures, Coatings

ABSTRACT

The use of an external mechanical pump to sustain the circulation in a body, also known as extracorporeal circulation, is an integral part of many medical procedures such as hemodialysis and cardio-pulmonary bypass. However, the damage to red blood cells caused by the flow-induced shear stresses in the flow circuit have remained an intractable problem for many years, limiting the operational duration of extracorporeal circulation. In this study, near-superhydrophobic surfaces were investigated as a potential solution to mitigate the hemolysis of blood during extracorporeal pumping through the use of a proof-of-concept flow circuit. It was found that the thin layer of air trapped by the near-superhydrophobic surface in the Cassie-Baxter state reduced the wall shear stress exerted on the blood flow, resulting in a corresponding decrease in the rate of hemolysis. For blood that undergoes an

1 oscillatory flow, this reduction in the hemolysis was shown to be directly related to
2 the mean shear rate and shear rate amplitude of the flow.

3

1 INTRODUCTION

2 Extracorporeal circulation, a process in which the circulation of blood in a body is
3 sustained with the aid of a mechanical pump in an external circuit, is crucial for medical
4 procedures such as cardiopulmonary bypass and hemodialysis¹⁻⁵. A major limitation of the
5 process, however, is that it introduces hemolysis (i.e. mechanical destruction of red blood
6 cells), which constrains the duration of its operation⁶⁻¹¹.

7 Although the main cause of this blood damage had already been ascertained to be the
8 shear stresses exerted on the blood as it flows through the extracorporeal circuit^{7,8,11,12}, few
9 solutions have been proposed to mitigate the hemolytic activities of the external pumping
10 circuit. Current research efforts aimed at lowering hemolysis rates are focused mainly on
11 developing low shear pump designs and optimizing operating parameters, such as rotation
12 speed, flow rate and pump head^{13,14}. The most practical and promising suggestion to date
13 involves lowering the occlusion level of roller pumps^{3,4}, a common extracorporeal circulation
14 pump. The reduction in hemolysis achieved using this technique, however, comes at the cost
15 of decreased flow rates and pumping inefficiency. In addition, it cannot be implemented for
16 centrifugal pumps, which have found widespread use in extracorporeal circulation as well^{2,9,15}.

17 All these limitations, however, can potentially be circumvented by the use of
18 superhydrophobic or near-superhydrophobic surface coatings in the extracorporeal circuit.
19 Such surfaces are highly water repellent, and generally depend on the deposition or
20 fabrication of hydrophobic micro- and/ or nano-structures on the surface to work¹⁶⁻²¹.
21 Because of the low surface energy of these structures, water or water-based solutions/
22 suspensions cannot seep in between the structures, but remain suspended and supported only
23 by the top of the structures²¹. As a result, the fluid effectively sits on a surface made up of air
24 and the top of the micro-/ nano-structures, which is also known as the Cassie-Baxter state^{22,23}.

1 Due to this unique arrangement, water droplets have very low adhesion to near-
2 superhydrophobic/ superhydrophobic surfaces and tend to roll or bounce off these surfaces
3 easily^{16,19,20}. In addition, it has been shown that near-superhydrophobic/ superhydrophobic
4 surfaces impart very low wall shear stresses to flowing fluids because it enabled deviations
5 from the “no-slip” flow condition of fluid near to the surfaces, thus allowing the same amount
6 of fluid to be delivered from one point to another using a lower pressure (i.e. improved
7 pumping efficiency)²⁴⁻²⁶. This diminished wall shear stress should, in theory, also lead to a
8 lower hemolysis rate when near-superhydrophobic/ superhydrophobic surfaces are
9 incorporated into an extracorporeal circuit.

10 The objective of this report, therefore, is to quantitatively characterize the hemolytic
11 potential of a near-superhydrophobic surface with respect to a regular surface, and relate the
12 observed difference to the reduction in wall shear stress induced by the near-
13 superhydrophobic surface by means of an established mathematical model. It should be
14 emphasized that the current report documents a proof-of-concept study and hence, the flow
15 circuit used for the experiments was not reflective of those currently employed by medical
16 professionals for actual extracorporeal circulation.

17

18

1 MATERIALS AND METHODS

2 Blood

3 Fresh porcine blood (Primary Industries Pte Ltd, Singapore) was obtained and used in
4 accordance to the rules and regulations of the Agri-Food and Veterinary Authority of
5 Singapore. Every 10 parts of the blood was mixed with 1 part of an anticoagulant to prevent
6 blood clots from forming. The anticoagulant was obtained by adding 1.975 g of sodium
7 citrate tribasic dihydrate (Sigma Aldrich C8532) and 1g of HEPES (Sigma Aldrich H3375)
8 for every 50 ml of deionized water.

9

10 Hematocrit Measurements

11 Blood samples in a 15ml test tube were separated into plasma and blood cells through
12 the use of the centrifuge, Sartorius Sigma 3-18K, at 9000 rpm for 5 minutes. The hematocrit
13 can be calculated as the volume ratio of blood cells to the entire blood sample.

14

15 Hemolysis Characterization

16 The degree of hemolysis was quantified by measuring the concentration of
17 hemoglobin in the blood plasma using a commercial hemoglobin assay kit (Sigma Aldrich
18 MAK115). 200 μ l of the hemoglobin assay reagent was first mixed with 50 μ l of blood
19 plasma, obtained the same way as that described for hematocrit measurements, and left to
20 incubate for 5 minutes at room temperature. The concentration of plasma hemoglobin was
21 then determined from absorbance measurements of the mixture at a wavelength of 400 nm,
22 using a spectrophotometric multiwall plate reader (Tecan Infinite M200 Pro). The damage to
23 the red blood cells were also qualitatively verified by acquiring optical microscopy images of
24 the red blood cells before and after they were subjected to extracorporeal pumping using
25 Olympus Microscope CX41.

1

2 Fabrication of Near-Superhydrophobic Surface

3 Near-superhydrophobic surfaces were obtained by depositing a commercial liquid
4 repellent coating²⁷ (Rust-Oleum Neverwet) on the inside of a PVC (polyvinyl chloride) pipe.
5 This was accomplished by first pouring the base coat solution of the Neverwet coating onto
6 the inside surface of a PVC pipe inclined at approximately 60° to the horizontal, and rotating
7 the pipe as the base coat dried to ensure an even coating. An hour after the application of the
8 base coat, the top coat was applied to the inside surface of the pipe in the same manner and
9 left to set for another hour.

10 PVC pipes were selected for this study as it had a similar hemolytic potential with the
11 polyurethane binder of the liquid repellent coating²⁸, ensuring that any difference in
12 hemolysis rates between the near-superhydrophobic and regular surfaces was caused solely
13 by surface roughness and not a result of dissimilar surface chemistry. Polyurethane tubes,
14 which are less rigid, were not used due to their tendency to flex and cause changes to the
15 diameter of the tube during pumping.

16

17 Surface Characterization

18 The wettability of the superhydrophobic surface and a regular PVC surface were
19 quantified using contact angle measurements of at least 5 different droplets for each type of
20 surface. Scanning electron microscopy (SEM) pictures were obtained using FEI Inspect F50
21 after the samples have been coated with 20 nm of aluminum by means of an Edwards Auto
22 360 thermal evaporator, in order to improve the electrical conductivity of the surface.
23 Surface roughness measurements were made using a surface profilometer, Alpha Step 500
24 (Tencor Instruments), at 4 different locations on the inside surface of a coated, as well as an

1 uncoated, PVC pipe. The pipes were sawn in half to facilitate the measurements. The
2 thickness of the coating was similarly measured by means of microscopy images.

3

4 Flow Loop

5 To generate mechanical damage to the blood in the extracorporeal circuit, a closed
6 flow loop containing about 800 ml of blood was used (Fig. 1a). The flow loop consists of an
7 open reservoir (blue), a flow probe (black), a rigid pipe with either a near-superhydrophobic
8 inner surface or regular PVC inner surface (gray), and a commercial medical pump (Kamoer
9 CK-15) which drove the blood flow. The pipe had a length of 30 cm, an inner diameter of 14
10 mm and a thickness of 2 mm, and connections between the various circuit elements were
11 made using elastic silicone tubes (yellow) with an inner diameter of 8 mm and a thickness of
12 2 mm. The total length of the silicone tubes was 1 m, which was sufficiently long to avoid the
13 formation of kinks in the tubes as they form a close loop in the circuit. PTFE tape were used,
14 where necessary, to prevent leaks. The flow probe was connected to a flow meter (Model 501,
15 Carolina Medical Electronics Inc.) and data acquisition unit (National Instruments, USB X
16 series) which sampled the real time flow rate at a frequency of 2000 Hz.

17 The medical pump is a fully occluded roller pump that provides pulsatile flow. It
18 works by squeezing the blood-filled silicone tube with a roller and moving the roller along
19 the elastic tube to push the fluid forward (Fig. 1b). As one roller finishes its course of motion
20 and releases the tube, another takes its place. In such pumps, the mean flow rate can only be
21 increased by raising the frequency of roller movement³.

22 The hemolytic performance of a near-superhydrophobic surface was investigated by
23 inserting a rigid pipe with the liquid repellent coating into the flow circuit. The coating was
24 applied to the inside of rigid PVC pipes rather than that of the elastic silicone tubes as the
25 latter tend to flex significantly during operation, which can cause spalling of the coating.

1 Blood was then driven through the circuit at different flow settings by systematically
2 increasing the roller frequency from 0 Hz to 15.7 Hz, the maximum setting on the pump. The
3 mean flow rate obtained using these frequencies covers the full spectrum of flow rates
4 commonly used in hemodialysis²⁹⁻³¹ and the lower end of spectrum used in cardiopulmonary
5 bypass surgeries^{32,33}. For the control experiments, the pipe with the liquid repellent coating
6 was replaced by a regular uncoated PVC pipe with everything else remaining constant, and
7 the experiments were repeated with the same flow settings. This ensured that any difference
8 in hemolysis observed between the variable and control experiments was due solely to the
9 flow over the different surfaces on the inside of the PVC pipes.

10 Each hemolysis experiment was carried out for 90 minutes under ambient conditions
11 (temperature = 20°C, relative humidity = 30%), with the pump running continuously for the
12 full duration. 15 ml blood samples were drawn from the flow loop and tested for plasma
13 hemoglobin at 30 minute intervals. Following the procedure of Noon *et. al.*¹, at least 3
14 different plasma hemoglobin readings were taken for each time point. Other than one outlier
15 at $t = 30$ min for the flow setting, VI (N.S.H), all the readings were included in the results
16 analysis.

17

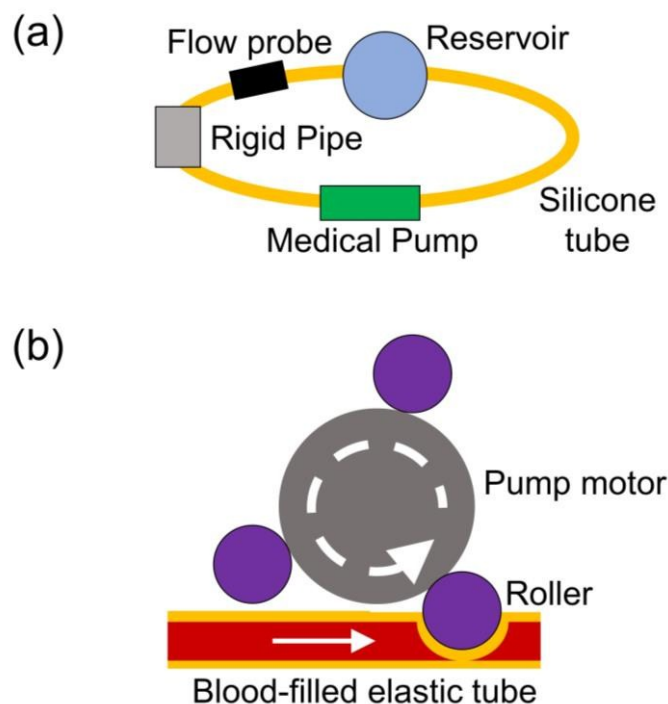


Figure 1: Schematic diagrams illustrating (a) the setup of the closed flow loop and (b) the operation of the medical roller pump with an elastic tube.

Computational Fluid Dynamic (CFD) Simulations

CFD simulations were carried out to evaluate the wall shear stresses exerted on the blood for each flow setting. This was done by modeling the pipe using 12000 axisymmetric elements in ANSYS Workbench (ANSYS, Inc., Canonsburg, PA, USA). The flow waveforms, obtained with the flow probe for different pump settings, were then applied at the pipe inlet as a boundary condition. The boundary condition for the outlet is pressure = 0 Pa and the no-slip boundary condition was applied to the pipe walls to simulate the PVC surface. Flow across the near-superhydrophobic surface cannot be simulated as easily, however, and therefore, the corresponding shear stresses will be calculated through analytical means, based on the simulation results for the PVC surface instead.

FLUENT 15.0 (ANSYS, Inc., Canonsburg, PA, USA) was used to perform the CFD simulations for 6 complete cycles (20 time steps/ cycle) of each flow waveform to remove the

1 transient effects and achieve steady state before the shear stresses on the model were acquired.
2 A non-Newtonian model (Carreau) was used for the dynamic viscosity of blood in the
3 simulations, which is given by³⁴

$$4 \quad \eta = \eta_{\infty} + (\eta_0 - \eta_{\infty}) \left[1 + (\lambda G)^2 \right]^{\frac{n-1}{2}} \quad (1)$$

5 where G refers to the shear rate, η_{∞} is the dynamic viscosity for a Newtonian model, 0.0035
6 Pas, η_0 is the dynamic viscosity at zero shear, 0.056 Pas, and λ and n are constants equivalent
7 to 3.31s and 0.357 respectively.

8

9

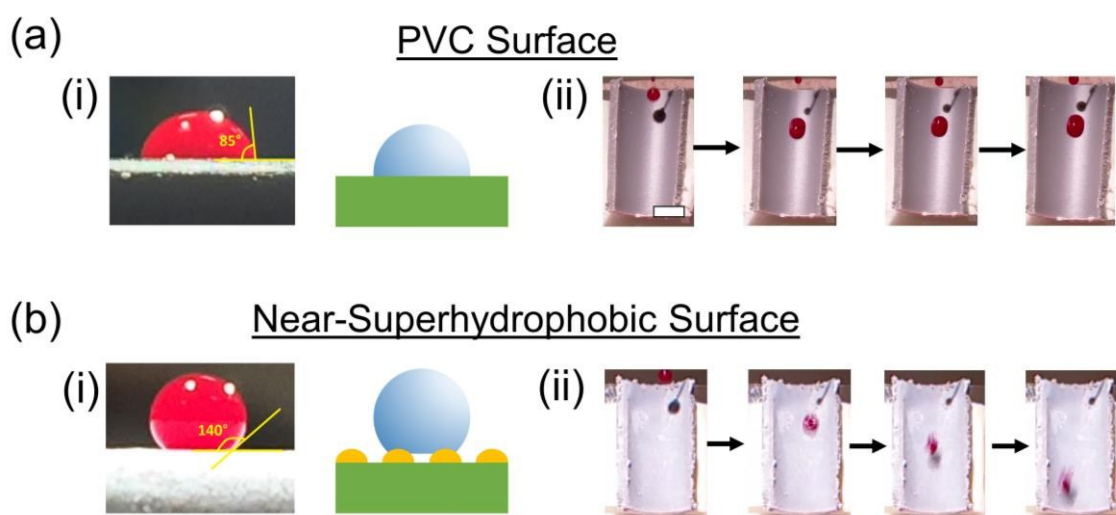
1 RESULTS

2 Near-Superhydrophobicity

3 The liquid repellent coating was found to cover the inner surface of the rigid pipe
 4 uniformly with a thickness of $53.0 \pm 6.7 \mu\text{m}$ and an average roughness of $2.34 \pm 1.07 \mu\text{m}$.
 5 This roughness was mostly due to the components within the liquid repellent coating and not
 6 imparted by the original, uncoated PVC surface which was comparatively smooth, with an
 7 average roughness of $0.21 \pm 0.12 \mu\text{m}$.

8 The coating works by creating a rough surface composed of silanized micro- and
 9 nano- particles embedded in a polyurethane matrix²⁷ (see Supplementary Information).
 10 Because of the highly hydrophobic nature of these particles, water was not able to imbibe the
 11 rough surface to wet the micro- and nano-structures, but instead, lie on the top of these
 12 structures on a composite surface of solid and air, which is also known as the Cassie-Baxter
 13 state. Additional experiments had been performed to demonstrate this, and can be found in
 14 the Supplementary Information.

15
 16



17

18 **Figure 2: (ai) Photo of a 6 μl blood droplet exhibiting a contact angle of 85° on a flat**
 19 **PVC surface and a schematic diagram illustrating the state of the droplet. (aii)**

1 **Sequential images showing the sticking and spreading of a 6 μ l blood droplet deposited**
2 **onto a PVC surface. (bi) Photo of a 6 μ l blood droplet exhibiting a contact angle of 140 $^{\circ}$**
3 **on a flat PVC surface with a near-superhydrophobic coating and a schematic diagram**
4 **illustrating the Cassie-Baxter state of the droplet. Green – PVC surface; Orange –**
5 **hydrophobic micro-/ nano- structures. (bii) Sequential images showing a 6 μ l blood**
6 **droplet bouncing off a near-superhydrophobic surface. Note that the pipes in (aii) and**
7 **(bii) were inclined at 45 $^{\circ}$ to the horizontal.**

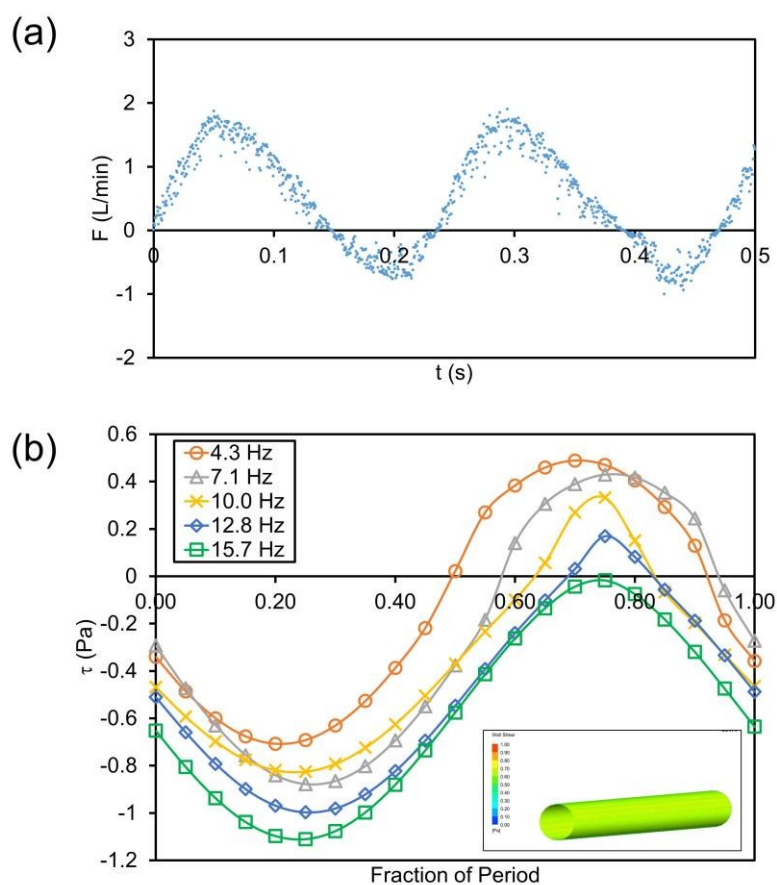
8
9 The effect of the liquid repellent coating on PVC can be seen in Fig. 2, where the
10 contact angle of a blood droplet can be observed to rise from 85.5 $^{\circ} \pm 3.2^{\circ}$ for a flat, regular
11 PVC surface to 140.6 $^{\circ} \pm 4.1^{\circ}$ for a flat, coated PVC surface. These values are close to contact
12 angle measurements obtained using water droplets (82.8 $^{\circ} \pm 2.5^{\circ}$ for PVC; 138.4 $^{\circ} \pm 3.0^{\circ}$ for
13 coated PVC).

14 Following scientific convention, the coated PVC surface is termed as near-
15 superhydrophobic, since superhydrophobic surfaces require the static contact angle to be
16 greater than an arbitrarily defined value of 150 $^{\circ}$ ^{18,35}. Nonetheless, it is worth noting that the
17 coated PVC surface displayed a high degree of non-wettability (roll-off angle/ contact angle
18 hysteresis $\approx 0^{\circ}$) and trapped liquid in the Cassie-Baxter state, which are characteristics of
19 superhydrophobic surfaces^{20,35}. Thus, the results of this study are not expected to differ
20 significantly even if a fully superhydrophobic surface had been used instead.

21 As further proof that the non-wetting property persisted even when the coating was on
22 the inside of the rigid pipe, pipes with and without the hydrophobic coating were sawn open
23 and 6 μ l of blood droplets were deposited onto them. The blood droplets were observed to
24 stick and spread out on the regular PVC surface (Fig. 2a_{ii}) but bounced off the near-
25 superhydrophobic coated surface rapidly (Fig. 2b_{ii}).

26

27

1 Flow Rates and Shear Stresses

2

3 **Figure 3: (a) Instantaneous flow rate detected by the flow probe for flow setting II. (b)**
 4 **Variation in wall shear stress for the different flow settings over a single period for the**
 5 **PVC surface obtained using CFD simulations. Note that the direction of net flow by the**
 6 **fluid is taken to be positive here. Since the shear stress exerted on the fluid by the pipe**
 7 **wall was always in the opposite direction to the flow, the average shear stresses are**
 8 **negative. (Inset) Representative CFD result showing the uniform spatial distribution of**
 9 **wall shear stress on the model of the pipe for flow setting VI.**

10

11 Fig. 3a shows a typical pulsatile flow waveform produced by the roller pump. The
 12 waveform is approximately sinusoidal, and can be expressed as

$$13 \quad F(t) = F_0 + F_a \sin \omega t \quad (2)$$

14 where $F(t)$ is the instantaneous flow rate, F_0 is the mean flow rate, F_a is the amplitude of flow,
 15 t is time and ω refers to the angular velocity of the flow, which is given by $2\pi f$ where f is the

1 frequency of the pulsatile waveforms generated by the rollers. The waveform was checked
 2 every 30 minutes during the experiments and were found to be stable and consistent for all
 3 flow settings.

4 Using the flow waveforms in CFD simulations, the instantaneous wall shear stress
 5 experienced by the PVC surface for each type of flow waveform was obtained. From Fig. 3b,
 6 it can be seen that the wall shear stress followed the sinusoidal character of the flow
 7 waveform, and was spatially uniform throughout the wall of the symmetrical PVC pipe (Fig.
 8 3b inset).

9 In addition, the magnitude of τ_0 , the mean wall shear stress, can be observed to
 10 increase with the mean flow rate, F_0 (see Table 1). The amplitude of the shear stress
 11 waveform, on the other hand, remained mostly the same, as the amplitude of the flow
 12 oscillations did not vary significantly for the different flow settings. The instantaneous wall
 13 shear stress can be given by

$$\tau(t) = \tau_0 + \tau_a \sin \omega t \quad (3)$$

14 where $\tau(t)$ is the instantaneous flow rate and τ_a is the amplitude of the oscillating shear stress.
 15 Table 1 documents the various properties of the different flow waveforms tested, including
 16 the shear rate values, G_0 and G_a , that correspond to the respective values of τ_0 and τ_a .

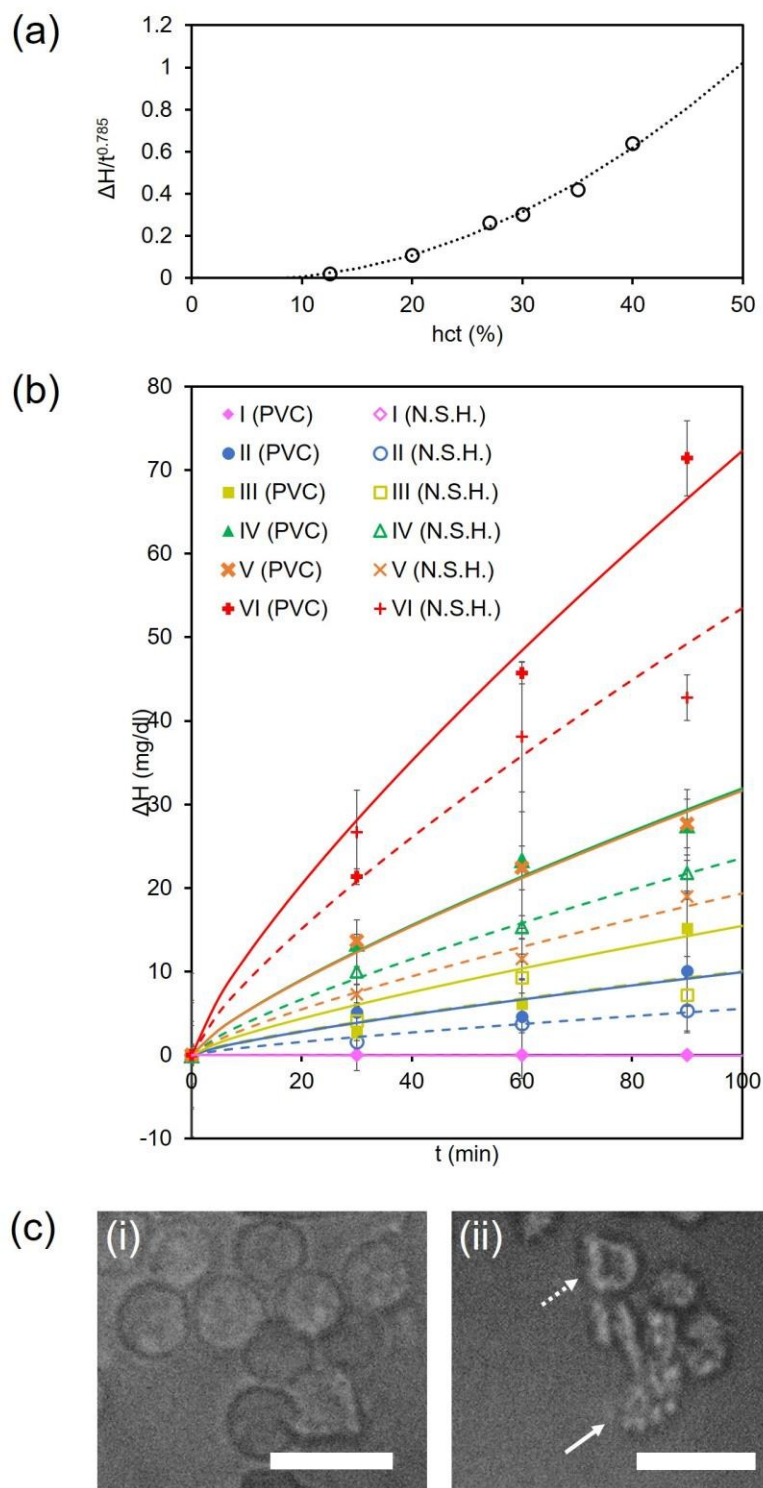
17
 18
 19 **Table 1: Parameters for the 6 different flow settings used. τ_0 and τ_a are tabulated based**
 20 **on data shown in Fig. 3b. Note that $G_0 = -\tau_0/\eta$ and $G_a = -\tau_a/\eta$.**

| Flow setting | I | II | III | IV | V | VI |
|---------------|------|-------|-------|-------|-------|-------|
| f (Hz) | 0.00 | 4.30 | 7.10 | 10.0 | 12.80 | 15.70 |
| F_0 (L/min) | 0.00 | 0.35 | 0.74 | 1.00 | 1.27 | 1.47 |
| F_a (L/min) | 0.00 | 0.97 | 1.07 | 0.79 | 0.94 | 1.00 |
| τ_0 (Pa) | 0.00 | -0.14 | -0.26 | -0.37 | -0.49 | -0.59 |

| | | | | | | |
|--------------------------|------|--------|--------|--------|--------|--------|
| G_0 (s ⁻¹) | 0.00 | 19.3 | 46.0 | 73.5 | 104 | 130.5 |
| τ_a (Pa) | 0.00 | 0.60 | 0.65 | 0.58 | 0.58 | 0.55 |
| G_a (s ⁻¹) | 0.00 | 131.50 | 145.70 | 126.30 | 127.50 | 118.00 |

1

2

1 Hemolysis

2

3 **Figure 4: (a) Plot of $\Delta H/t^{0.785}$ vs. hct . The data points represent the experimentally**
 4 **measured values while the dotted trend line represents Eq. 4. (b) Plot of ΔH vs. t for the**
 5 **different flow settings. The data points represent experimentally measured values while**
 6 **the trend lines represent the best fit curves of the data points to the relationship of $\Delta H \propto$**

1 $t^{0.785}$. The best fit curve and data points for the same flow setting are given the same
 2 color. Best fit curves of the near-superhydrophobic surface (N.S.H) are represented by
 3 dashed lines whereas that of the regular PVC surface are represented by solid lines. The
 4 units for ΔH and t are mg/dl and min respectively. Error bars represent standard
 5 deviations. (c) Bright field optical microscopy images of red blood cells (i) before and (ii)
 6 after being subjected to extracorporeal pumping through a regular PVC pipe at flow
 7 setting VI for 60 min. The dotted white arrow points to a red blood cell with deformed
 8 cell membrane while the solid white arrow points to a red blood cell with spiky
 9 protrusions. Scale bars represent 10 μm .

10
 11 It is known that the level of hematocrit present in the blood influences the rate of
 12 hemolysis³⁶ and thus, normalization had to be carried out to ensure a fair comparison between
 13 the results of the experiments. To do so, blood of different hematocrit levels, achieved by
 14 diluting the blood with phosphate buffered solution (1X), were subjected to the same flow
 15 condition (flow setting III) in the experimental setup for 60 minutes. The plasma hemoglobin
 16 for each sample was then measured and plotted in Fig. 4a to obtain the normalization curve. It
 17 was found that for the range of hematocrit tested, the rate of increase of plasma hemoglobin
 18 ($\Delta H/t^{0.785}$, in mg/dl.min^{0.785}) is a quadratic function of hematocrit (hct , in %),

$$19 \quad \Delta H / t^{0.785} = 0.0005(hct)^2 - 0.0047(hct) \quad (4)$$

20 Note that the units of the constants, 0.0005 and 0.0047, in Eq. (4) can be shown to be
 21 mg/dl.min^{0.785} by balancing the scientific units on both sides of the equation.

22 Using eq. (4), the concentration of plasma hemoglobin at each time point for the
 23 different experiments were then adjusted to a hematocrit of 40% (average hematocrit of all
 24 samples = 38.2% \pm 8.6%) and plotted as data points in Fig. 4b. Data for Fig. 4b in the
 25 tabulated form can be found in the Supplementary Information. The magnitude of ΔH is
 26 consistent with those reported for similar experiments¹, providing validation for our results. It
 27 had also been shown previously³⁷ that ΔH is proportional to $t^{0.785}$, and it can be observed that

1 the data points fit closely to this trend, indicated as dashed lines (near-superhydrophobic
2 surface) and solid lines (PVC surface) in Fig. 4b, with an average R^2 value of 0.92 ± 0.08 .
3 However, because of the low levels of hemolysis involved, the $\Delta H \propto t^{0.785}$ fitting was
4 statistically insignificant ($p > 0.05$) for the cases I (PVC), II (PVC), III (PVC), I (N.S.H) and
5 II (N.S.H).

6 While it may be surprising that the hemolysis rate for both the PVC surface and liquid
7 repellent coating were found to follow the same power law, despite being of different surface
8 chemistry, this is to be expected, as Offeman and Williams had previously established that
9 polyurethane, the polymeric binder in the coating, exhibited similar hemolytic kinetics as
10 PVC²⁸, which Lampert and Williams³⁸ had determined to be approximately $\Delta H \propto t^{0.785}$.

11 From Fig. 4b, it can be observed that the rate of hemolysis, indicated by the gradient
12 of the trend lines, was always greater for regular PVC surfaces as compared to near-
13 superhydrophobic surfaces for any given flow condition, other than flow setting I (no flow;
14 static condition). For flow setting I, there was no discernible increment in ΔH over time for
15 both the near-superhydrophobic and PVC surfaces, implying that there were no chemical
16 reactions between the blood with the PVC or liquid repellent coating that led to hemolysis i.e.
17 the PVC surface and liquid repellent coating were biocompatible and not toxic to blood³⁹.

18 To account for the difference in hemolysis rates between regular and near-
19 superhydrophobic surfaces, the mechanical force acting on the blood flow, which is a well-
20 known source of hemolysis^{7,8,11}, was examined. It was found that for the experimental
21 parameters of this study, hydrodynamic pressure was not the cause for hemolysis. This is
22 because Blackshear *et al.*⁷ had previously shown that hemolysis only takes place if the
23 pressure, relative to the atmosphere, is greater than 2000 mmHg, but in all the experiments
24 performed for this study, the hydrodynamic pressure did not even exceed 50 mmHg (see
25 Supplementary Information).

1 In addition, it can be observed from Fig. 4b that the hemolysis rates generally rise
2 from flow setting I to VI, which is associated with increased mean flow rates and higher wall
3 shear stresses (Table 1 and Fig. 3b). This is consistent with previous studies which showed
4 that exposure to shear stresses can lead to red blood cell damage^{7,8,11}. To further confirm this,
5 the microscopy images of the red blood cells before and after being subjected to
6 extracorporeal pumping were examined. From Fig. 4c, it can be seen that after extracorporeal
7 circulation, the red blood cell membranes were deformed (dotted arrow in Fig. 4cii) or had
8 spiky protrusions (solid arrow in Fig. 4cii), a phenomenon that was also observed in previous
9 studies⁴⁰ detailing the effects of shear stresses on red blood cell damage (see Supplementary
10 Information for more microscopy images of the damaged red blood cells). These evidence
11 indicate that shear stresses were the main cause behind the hemolysis observed in the
12 experiments.

13 Furthermore, for the sake of completeness, we also examine the possibility that the
14 liquid repellent coating on the near-superhydrophobic surface may have chemically
15 strengthened the red blood cells against shear stresses and caused a reduction in the rate of
16 hemolysis during flow. While our experiments do not preclude the potential of this happening,
17 the likelihood is extremely low for the following reasons.

18 Firstly, to the best of our knowledge, there has been no report on any polymer or
19 ceramic that can improve the resistance of red blood cells to hemolysis during blood flow.
20 This is also true for nanoparticles, which have only been shown to be capable of inducing
21 hemolysis, rather than strengthen red blood cells against damage⁴¹⁻⁴³. Lastly, if the coating
22 had chemically reacted with the red blood cells, some level of degradation should have taken
23 place. However, there were no observed changes to the appearance and performance of the
24 liquid repellent coating throughout the study. In fact, the blood contact angle of the near-

1 superhydrophobic surface after a hemolysis experiment was measured to be $139.5^\circ \pm 4.1^\circ$,
 2 which is nearly identical to the pre-experimental value of $140.6^\circ \pm 4.1^\circ$.

3 Therefore, it is most likely that the difference in hemolysis rates observed between the
 4 near-superhydrophobic and PVC surfaces is solely due to dissimilar wall shear stresses
 5 exerted on the blood flow by the respective surfaces. To validate this, our results will be
 6 quantitatively analyzed and compared to well-established models that describe shear-induced
 7 hemolysis in the following section.

8

9 DISCUSSION

10 Considering the hemolysis of blood in the experimental setup shown in Fig. 1a was
 11 caused by wall shear stresses generated by the flow of blood through the rigid pipe and the
 12 rest of the circuit,

$$13 \quad \Delta H_{PVC} = \Delta H_{p,PVC} + \Delta H_r \quad (5)$$

$$14 \quad \Delta H_{N.S.H} = \Delta H_{p,N.S.H} + \Delta H_r \quad (6)$$

15 where ΔH is the total increase in plasma hemoglobin, ΔH_p is the increase in plasma
 16 hemoglobin due to the flow through the rigid pipe and ΔH_r is the increase in plasma
 17 hemoglobin due to the flow through the rest of the circuit. The subscripts PVC and N.S.H.
 18 (near-superhydrophobic) denote the surface that the respective variables belong to. From eq.
 19 (5) and (6), the reduction in hemolysis enabled by the near-superhydrophobic coating, ΔH_c ,
 20 can be isolated as

$$21 \quad \Delta H_c = \Delta H_{PVC} - \Delta H_{N.S.H} = \Delta H_{p,PVC} - \Delta H_{p,N.S.H} \quad (7)$$

22 Arora *et. al.*¹² had previously used a strain-based approach, built on Giersiepen *et.*
 23 *al.*'s work³⁷, to develop a prediction for the hemolysis of blood subjected to a low-intensity
 24 oscillating flow. In this model, the viscoelastic character of the red blood cell membrane is
 25 taken into account and its failure is brought about when the red blood cell becomes critically

1 deformed. This distortion to the shape of the red blood cell in a pulsatile flow is influenced by
 2 G_0 and G_a , which determine the maximum, minimum and net deformation of the red blood
 3 cell (Fig. 5a). Within the parameters of this study, the mathematical model can approximately
 4 be expressed as¹²

$$\Delta H_{p,PVC} = kG_0^{2.4} \beta^{1.6} t^{0.785} \quad (8)$$

6 where k is a proportionality constant that takes into account all other factors influencing
 7 hemolysis and $\beta = G_a/G_0$. Note that $G_0 = -\tau_0/\eta$ and $G_a = -\tau_a/\eta$. The values of G_a and G_0 can
 8 be computed from Fig. 3b and are documented in Table 1.

9 It was also shown previously by Ou *et. al.*²⁴ that the reduced shear stress experienced
 10 by fluids flowing past near-superhydrophobic/ superhydrophobic surfaces is a direct result of
 11 the diminished area of contact between the fluid and solid surface, due to the thin layer of air
 12 trapped by the hydrophobic surface roughness. In other words, the fluid in the blood, as well
 13 as red blood cells, was effectively flowing past shear-free fluid-air interfaces as well as fluid-
 14 solid interfaces where the no-slip boundary condition persisted. Therefore,

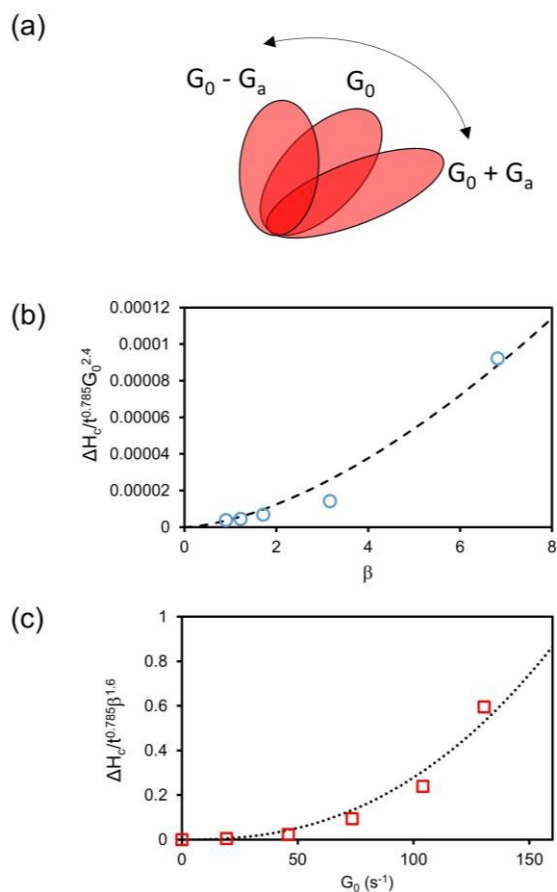
$$\Delta H_{p,N.S.H} = mkG_0^{2.4} \beta^{1.6} t^{0.785} \quad (9)$$

16 where m is the fraction of the inner surface area of the coated pipe that is in direct contact
 17 with the fluid. The value of m can be computed for orderly arrays of micro-/nano- structures²⁰
 18 or measured using techniques such as Raman spectroscopy for disorderly surface roughness⁴⁴.

19 Substituting Eq. (8) and Eq. (9) into Eq. (7), it can be shown that

$$\Delta H_c = KG_0^{2.4} \beta^{1.6} t^{0.785} \quad (10)$$

21 where $K = (1-m)k$. It is worth noting that Eq. (10) predicts that the reduction in hemolysis
 22 brought about by a near-superhydrophobic surface is expected to increase with higher G_0 and
 23 β .



1
2 **Figure 5: (a) Schematic diagrams illustrating the deformation of a red blood**
3 **cell subjected to the minimum shear rate, $G_0 - G_a$ and the maximum shear rate, $G_0 + G_a$, of a**
4 **pulsatile flow. The cell oscillates between these shapes so that its net deformation is**
5 **given by the average shear rate, G_0 . (b) Plot of $\Delta H_c / G_0^{2.4} t^{0.785}$ vs. β . The dashed trend line**
6 **represents the relationship $\Delta H_c / G_0^{2.4} t^{0.785} \propto \beta^{1.6}$. (c) Plot of $\Delta H_c / \beta^{1.6} t^{0.785}$ vs. G_0 . The**
7 **dotted trend line represents the relationship $\Delta H_c / \beta^{1.6} t^{0.785} \propto G_0^{2.4}$. For (b) and (c), each**
8 **data point represents 1 flow setting. The units for ΔH_c , G_0 and t are mg/dl, s^{-1} and min**
9 **respectively.**

10

11 To verify our analysis, the experimentally obtained values of $\Delta H_c / t^{0.785}$ for each flow
12 setting were first computed using

13
$$\frac{\Delta H_c}{t^{0.785}} = \frac{\Delta H_{p,PVC}}{t^{0.785}} - \frac{\Delta H_{p,N.S.H.}}{t^{0.785}} \quad (11)$$

Eq. (11) can be derived from Eq. (7). The values of $\Delta H_{p,PVC}/t^{0.785}$ and $\Delta H_{p,N.S.H.}/t^{0.785}$ for each flow setting can be found using the proportionality constant of the trend lines shown in Fig. 4b. Then, using the values of G_0 and β for each flow setting, $\Delta H_c/G_0^{2.4}t^{0.785}$ vs. β and $\Delta H_c/\beta^{1.6}t^{0.785}$ vs. G_0 were plotted as data points in Fig. 5b and 5c respectively.

Since Eq. (10) can be re-written as

$$\Delta H_c / G_0^{2.4}t^{0.785} = K\beta^{1.6} \quad (12),$$

the $\Delta H_c/G_0^{2.4}t^{0.785}$ vs. β data points in Fig. 5b must adhere closely to the power-law trend of $y \propto x^{1.6}$ (represented by the dashed line in Fig. 5b) for Eq. (10) to be valid. Similarly, Eq. (10) can also be re-written as

$$\Delta H_c / \beta^{1.6}t^{0.785} = KG_0^{2.4} \quad (13),$$

and for it to be valid, the $\Delta H_c/\beta^{1.6}t^{0.785}$ vs. G_0 data points in Fig. 5c must follow the power-law trend of $y \propto x^{2.4}$ (represented by the dotted line in Fig. 5c) closely. Moreover, the proportionality constant of the fitted trend lines in both Fig. 5b and Fig. 5c should give the same value for K as indicated in Eq. (12) and Eq. (13).

From Fig. 5b and 5c, it can be observed that the data points do indeed fit the expected trend lines. The R^2 value of fit for Fig. 5b was 0.97 while the R^2 value of fit for Fig. 5c was 0.96. Furthermore, the value of the proportionality constant, K , derived separately from the trend lines in Fig. 5b and 5c, was found to be equivalent to 4.1×10^{-6} in both plots. Fig. 5b and 5c, therefore, provide strong validation for the above analysis, which demonstrates that the lower hemolysis rates found on the near-superhydrophobic surface can be sufficiently accounted for by considering the diminished shear stresses brought about by the reduced contact area on such surfaces.

1 CONCLUSION

2 The hemolytic potential of near-superhydrophobic surfaces had been investigated and
3 found to be much lower than that of regular surfaces. This result was attributed to diminished
4 contact of the blood with the walls of the pipe due to a thin layer of air trapped by the near-
5 superhydrophobic surface, leading to reduced wall shear stresses acting on red blood cells
6 during extracorporeal circulation. In addition, it was shown through a detailed analysis of the
7 results that near-superhydrophobic surfaces provide a greater reduction of hemolysis when
8 the blood is subjected to more adverse flow conditions (higher mean shear rate and higher
9 shear rate amplitude). These results suggest that near-superhydrophobic surfaces may be
10 useful for reducing hemolysis when incorporated into extracorporeal circuits.

11

12 AUTHOR INFORMATION

13 Corresponding Author

14 *Email: laicq@mit.edu

15 Notes

16 The authors declare that there are no competing financial interests.

17

18 ACKNOWLEDGEMENTS

19 This study was partially supported by the Singapore Millennium Foundation (Grant number:
20 R-397-000-200-592; PI: Yap Choon Hwai). We thank Mr. Ivan Loh for his advice and
21 guidance on the use of the plasma hemoglobin test kit.

22

23

24

25

1 **REFERENCES**

- 2 (1) Noon, G. P.; Kane, L. E.; Feldman, L.; Peterson, J. A.; DeBakey, M. E. Reduction of
3 Blood Trauma in Roller Pumps for Long-Term Perfusion. *World J. Surg.* **1985**, *9* (1),
4 65–71.
- 5 (2) Rawn, D. J.; Harris, H. K.; Riley, J. B.; Yoda, D. N.; Blackwell, M. M. An under-
6 Occluded Roller Pump Is Less Hemolytic than a Centrifugal Pump. *J. Extra. Corpor.*
7 *Technol.* **1997**, *29* (1), 15–18.
- 8 (3) Tamari, Y.; Lee-Sensiba, K.; Leonard, E. F.; Tortolani, A. J. A Dynamic Method for
9 Setting Roller Pumps Nonocclusively Reduces Hemolysis and Predicts Retrograde
10 Flow. *ASAIO J. Am. Soc. Artif. Intern. Organs* 1992 **1997**, *43* (1), 39–52.
- 11 (4) Tayama, E.; Teshima, H.; Takaseya, T.; Fukunaga, S.; Tayama, K.; Hayashida, N.;
12 Akashi, H.; Kawara, T.; Aoyagi, S. Non-Occlusive Condition with the Better-Header
13 Roller Pump: Impacts of Flow Dynamics and Hemolysis. *Ann. Thorac. Cardiovasc.*
14 *Surg. Off. J. Assoc. Thorac. Cardiovasc. Surg. Asia* **2004**, *10* (6), 357–361.
- 15 (5) Reul, H. M.; Akdis, M. Blood Pumps for Circulatory Support. *Perfusion* **2000**, *15* (4),
16 295–311.
- 17 (6) Polaschegg, H.-D. Red Blood Cell Damage from Extracorporeal Circulation in
18 Hemodialysis. *Semin. Dial.* **2009**, *22* (5), 524–531.
- 19 (7) Blackshear, P. L.; Dorman, F. D.; Steinbach, J. H. SOME MECHANICAL EFFECTS
20 THAT INFLUENCE HEMOLYSIS. *Trans. - Am. Soc. Artif. Intern. Organs* **1965**, *11*,
21 112–117.
- 22 (8) Boehning, F.; Mejia, T.; Schmitz-Rode, T.; Steinseifer, U. Hemolysis in a Laminar
23 Flow-Through Couette Shearing Device: An Experimental Study. *Artif. Organs* **2014**,
24 *38* (9), 761–765.

- 1 (9) Byrnes, J.; McKamie, W.; Swearingen, C.; Proadhan, P.; Bhutta, A.; Jaquiss, R.;
2 Imamura, M.; Fiser, R. Hemolysis During Cardiac Extracorporeal Membrane
3 Oxygenation: A Case-Control Comparison of Roller Pumps and Centrifugal Pumps in
4 a Pediatric Population: *ASAIO J.* **2011**, *57* (5), 456–461.
- 5 (10) Ding, J.; Niu, S.; Chen, Z.; Zhang, T.; Griffith, B. P.; Wu, Z. J. Shear-Induced
6 Hemolysis: Species Differences. *Artif. Organs* **2015**, *39* (9), 795–802.
- 7 (11) Laugel, J. F.; Beissinger, R. L. Low Stress Shear-Induced Hemolysis in Capillary Flow.
8 *Trans. - Am. Soc. Artif. Intern. Organs* **1983**, *29*, 158–162.
- 9 (12) Arora, D.; Behr, M.; Pasquali, M. A Tensor-Based Measure for Estimating Blood
10 Damage. *Artif. Organs* **2004**, *28* (11), 1002–1015.
- 11 (13) Anai, H.; Nakatani, T.; Wakisaka, Y.; Araki, K.; Taenaka, Y.; Tatsumi, E.; Masuzawa,
12 T.; Baba, Y.; Eya, K.; Toda, K. An Approach to Reducing Hemolysis in an Axial-Flow
13 Blood Pump. *ASAIO J. Am. Soc. Artif. Intern. Organs* 1992 **1995**, *41* (3), M771-774.
- 14 (14) Park, M.; Mendes, P. V.; Hirota, A. S.; dos Santos, E. V.; Costa, E. L. V.; Azevedo, L.
15 C. P. Blood Flow/pump Rotation Ratio as an Artificial Lung Performance Monitoring
16 Tool during Extracorporeal Respiratory Support Using Centrifugal Pumps. *Rev. Bras.*
17 *Ter. Intensiva* **2015**, *27* (2), 178–184.
- 18 (15) Hansbro, S. D.; Sharpe, D. A.; Catchpole, R.; Welsh, K. R.; Munsch, C. M.;
19 McGoldrick, J. P.; Kay, P. H. Haemolysis during Cardiopulmonary Bypass: An in
20 Vivo Comparison of Standard Roller Pumps, Nonocclusive Roller Pumps and
21 Centrifugal Pumps. *Perfusion* **1999**, *14* (1), 3–10.
- 22 (16) Zhai, L.; Berg, M. C.; Cebeci, F. C.; Kim, Y.; Milwid, J. M.; Rubner, M. F.; Cohen, R.
23 E. Patterned Superhydrophobic Surfaces: Toward a Synthetic Mimic of the Namib
24 Desert Beetle. *Nano Lett.* **2006**, *6* (6), 1213–1217.

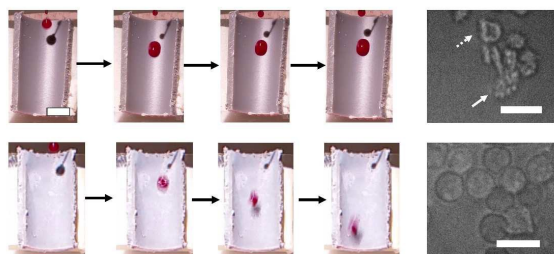
- 1 (17) Zheng, Y.; Gao, X.; Jiang, L. Directional Adhesion of Superhydrophobic Butterfly
2 Wings. *Soft Matter* **2007**, *3*, 178.
- 3 (18) Martines, E.; Seunarine, K.; Morgan, H.; Gadegaard, N.; Wilkinson, C. D. W.; Riehle,
4 M. O. Superhydrophobicity and Superhydrophilicity of Regular Nanopatterns. *Nano*
5 *Lett.* **2005**, *5* (10), 2097–2103.
- 6 (19) Dawood, M. K.; Zheng, H.; Kurniawan, N. A.; Leong, K. C.; Foo, Y. L.; Rajagopalan,
7 R.; Khan, S. A.; Choi, W. K. Modulation of Surface Wettability of Superhydrophobic
8 Substrates Using Si Nanowire Arrays and Capillary-Force-Induced Nanocoherence. *Soft*
9 *Matter* **2012**, *8* (13), 3549–3557.
- 10 (20) Lai, C. Q.; Cheng, H. Versatile Fabrication and Applications of Dense, Orderly Arrays
11 of Polymeric Nanostructures over Large Areas. *J. Mater. Chem. B* **2014**, *2* (36), 5982–
12 5991.
- 13 (21) Quéré, D. Surface Chemistry: Fakir Droplets. *Nat. Mater.* **2002**, *1* (1), 14–15.
- 14 (22) Cassie, A. B. D.; Baxter, S. Wettability of Porous Surfaces. *Trans. Faraday Soc.* **1944**,
15 *40*, 546.
- 16 (23) Choi, W.; Tuteja, A.; Mabry, J. M.; Cohen, R. E.; McKinley, G. H. A Modified Cassie-
17 Baxter Relationship to Explain Contact Angle Hysteresis and Anisotropy on Non-
18 Wetting Textured Surfaces. *J. Colloid Interface Sci.* **2009**, *339* (1), 208–216.
- 19 (24) Ou, J.; Perot, B.; Rothstein, J. P. Laminar Drag Reduction in Microchannels Using
20 Ultrahydrophobic Surfaces. *Phys. Fluids 1994-Present* **2004**, *16* (12), 4635–4643.
- 21 (25) Henoeh, C.; Krupenkin, T. N.; Kolodner, P.; Taylor, J. A.; Hodes, M. S.; Lyons, A. M.;
22 Peguero, C.; Breuer, K. Turbulent Drag Reduction Using Superhydrophobic Surfaces;
23 American Institute of Aeronautics and Astronautics: San Francisco, California, 2006.
- 24 (26) Daniello, R. J.; Waterhouse, N. E.; Rothstein, J. P. Drag Reduction in Turbulent Flows
25 over Superhydrophobic Surfaces. *Phys. Fluids 1994-Present* **2009**, *21* (8), 85103.

- 1 (27) BLEECHER, D.; Harsh, P.; Hurley, M.; Jones, A. K.; Ross, R.; Sikka, V. K.; Zielke, D.
2 Highly Durable Superhydrophobic, Oleophobic and Anti-Icing Coatings and Methods
3 and Compositions for Their Preparation. US9067821 B2, June 30, 2015.
- 4 (28) Offeman, R. D.; Williams, M. C. Material Effects in Shear-Induced Hemolysis.
5 *Biomater. Med. Devices Artif. Organs* **1979**, 7 (3), 359–391.
- 6 (29) Azar, A. T. Increasing Dialysate Flow Rate Increases Dialyzer Urea Clearance and
7 Dialysis Efficiency: An in Vivo Study. *Saudi J. Kidney Dis. Transplant. Off. Publ.*
8 *Saudi Cent. Organ Transplant. Saudi Arab.* **2009**, 20 (6), 1023–1029.
- 9 (30) Borzou, S. R.; Gholyaf, M.; Zandiha, M.; Amini, R.; Goodarzi, M. T.; Torkaman, B.
10 The Effect of Increasing Blood Flow Rate on Dialysis Adequacy in Hemodialysis
11 Patients. *Saudi J. Kidney Dis. Transplant. Off. Publ. Saudi Cent. Organ Transplant.*
12 *Saudi Arab.* **2009**, 20 (4), 639–642.
- 13 (31) Hassell, D. R.; van der Sande, F. M.; Kooman, J. P.; Tordoir, J. P.; Leunissen, K. M.
14 Optimizing Dialysis Dose by Increasing Blood Flow Rate in Patients with Reduced
15 Vascular-Access Flow Rate. *Am. J. Kidney Dis. Off. J. Natl. Kidney Found.* **2001**, 38
16 (5), 948–955.
- 17 (32) Alston, R. P.; Singh, M.; McLaren, A. D. Systemic Oxygen Uptake during
18 Hypothermic Cardiopulmonary Bypass. Effects of Flow Rate, Flow Character, and
19 Arterial pH. *J. Thorac. Cardiovasc. Surg.* **1989**, 98 (5 Pt 1), 757–768.
- 20 (33) Del Canale, S.; Vezzani, A.; Belli, L.; Coffrini, E.; Guariglia, A.; Ronda, N.; Vitali, P.;
21 Beghi, C.; Fesani, F.; Borghetti, A. A Comparative Clinical Study on the Effects of
22 Cardiopulmonary Bypass with Different Flows and Pressures on Skeletal Muscle Cell
23 Metabolism in Patients Undergoing Coronary Bypass Grafting. *J. Thorac. Cardiovasc.*
24 *Surg.* **1990**, 99 (2), 327–334.

- 1 (34) Siebert, M. W.; Fodor, P. S. Newtonian and Non-Newtonian Blood Flow over a
2 Backward-Facing Step - A Case Study. In *Proceedings of the COMSOL Conference*;
3 Boston, 2009.
- 4 (35) Öner, D.; McCarthy, T. J. Ultrahydrophobic Surfaces. Effects of Topography Length
5 Scales on Wettability. *Langmuir* **2000**, *16* (20), 7777–7782.
- 6 (36) Mizuguchi, K.; Damm, G. A.; Aber, G. S.; Bozeman, R. J.; Bacak, J. W.; Svejksky,
7 P. A.; Orime, Y.; Ohara, Y.; Naito, K.; Tasai, K. Does Hematocrit Affect in Vitro
8 Hemolysis Test Results? Preliminary Study with Baylor/NASA Prototype Axial Flow
9 Pump. *Artif. Organs* **1994**, *18* (9), 650–656.
- 10 (37) Giersiepen, M.; Wurzinger, L. J.; Opitz, R.; Reul, H. Estimation of Shear Stress-
11 Related Blood Damage in Heart Valve Prostheses--in Vitro Comparison of 25 Aortic
12 Valves. *Int. J. Artif. Organs* **1990**, *13* (5), 300–306.
- 13 (38) Lampert, R. H.; Williams, M. C. Effect of Surface Materials on Shear-Induced
14 Hemolysis. *J. Biomed. Mater. Res.* **1972**, *6* (6), 499–532.
- 15 (39) Ye, W.; Shi, Q.; Hou, J.; Jin, J.; Fan, Q.; Wong, S.-C.; Xu, X.; Yin, J.
16 Superhydrophobic Coating of Elastomer on Different Substrates Using a Liquid
17 Template to Construct a Biocompatible and Antibacterial Surface. *J. Mater. Chem. B*
18 **2014**, *2* (41), 7186–7191.
- 19 (40) Ding, M. J.; Xu, S. W.; Zhang, J.; Wang, Q.; Chang, Y.; Chen, F.; Zeng, Y. J. Trauma
20 to Erythrocytes Induced by Long Term in Vitro Pumping Using a Roller Pump. *Cell*
21 *Biol. Int.* **2007**, *31* (8), 763–767.
- 22 (41) Aseichev, A. V.; Azizova, O. A.; Beckman, E. M.; Skotnikova, O. I.; Dudnik, L. B.;
23 Shcheglovitova, O. N.; Sergienko, V. I. Effects of Gold Nanoparticles on Erythrocyte
24 Hemolysis. *Bull. Exp. Biol. Med.* **2014**, *156* (4), 495–498.

- 1 (42) Barshtein, G.; Arbell, D.; Yedgar, S. Hemolytic Effect of Polymeric Nanoparticles:
2 Role of Albumin. *IEEE Trans. NanoBioscience* **2011**, *10* (4), 259–261.
- 3 (43) Vinardell, M. P.; Sordé, A.; Díaz, J.; Baccarin, T.; Mitjans, M. Comparative Effects of
4 Macro-Sized Aluminum Oxide and Aluminum Oxide Nanoparticles on Erythrocyte
5 Hemolysis: Influence of Cell Source, Temperature, and Size. *J. Nanoparticle Res.*
6 **2015**, *17* (2), 1–10.
- 7 (44) Truong, V. K.; Webb, H. K.; Fadeeva, E.; Chichkov, B. N.; Wu, A. H. F.; Lamb, R.;
8 Wang, J. Y.; Crawford, R. J.; Ivanova, E. P. Air-Directed Attachment of Coccoid
9 Bacteria to the Surface of Superhydrophobic Lotus-like Titanium. *Biofouling* **2012**, *28*
10 (6), 539–550.
11

TABLE OF CONTENTS



Near-superhydrophobic surfaces trap circulating blood in Cassie-Baxter state, thereby reducing the contact area available for shearing of erythrocytes to take place.